Performance analysis of a plasmonic sensor based on gold nanoparticle film in infrared light using the admittance loci method

Kaushik Brahmachari and Mina Ray

Citation: Journal of Applied Physics **117**, 083110 (2015); doi: 10.1063/1.4913604
View online: http://dx.doi.org/10.1063/1.4913604
View Table of Contents: http://scitation.aip.org/content/aip/journal/jap/117/8?ver=pdfcov
Published by the AIP Publishing

Performance analysis of a plasmonic sensor based on gold nanoparticle film in infrared light using the admittance loci method

Kaushik Brahmachari and Mina Ray[a)]
Department of Applied Optics and Photonics, University of Calcutta, Technology Campus, Acharya Prafulla Chandra Roy Shiksha Prangan, JD-2, Sector-III, Salt Lake City, Kolkata 700 098, India

(Received 21 July 2014; accepted 15 February 2015; published online 27 February 2015)

A theoretical design of surface plasmon resonance (SPR) structure operating in attenuated total reflection (ATR) mode and comprising of silicon or chalcogenide (2S2G) prism material coated with gold film having different nanoparticle sizes has been reported along with some interesting performance related simulation results at the operating wavelength of 1200 nm in infrared. The admittance loci based technique has been employed for the appropriate choice of the metal layer thickness. The sensitivity and other performance parameters of the structure based on the choice of the high index prism material and correct gold nanoparticle size have also been presented. In comparison to other conventional prism based plasmonic structures, the proposed model provides the extra degree of freedom, i.e., variations of nanoparticle size in addition to the variation in layer thickness and the use of different high index prism materials like silicon, 2S2G materials, etc. Moreover, the width of the SPR curve can be controlled by using different high index prism materials as well as by changing gold nanoparticle size. Higher sensitivity can be achieved with 2S2G while higher detection accuracy is provided by silicon as prism material. © *2015 AIP Publishing LLC*.
[http://dx.doi.org/10.1063/1.4913604]

I. INTRODUCTION

Surface plasmon resonance (SPR) phenomenon occurs in a plasmonic structure due to the interaction of the p-polarized incident light with surface plasmon wave, which propagates along the metal-dielectric interface. The basic prism based configurations of plasmonic structure were proposed a long before for observing surface plasmon resonance.[1,2] The sensing capability of SPR phenomenon was first reported for gas detection and biosensing in 1983.[3] A theoretical investigation on sensitivity comparison of prism and grating coupler based plasmonic sensors in angular as well as in wavelength interrogation modes has been reported by Homola *et al.*[4] Optical properties of the metals have been explored in detail in the literature.[5] Excitation of surface plasmons using infrared light provides extra advantages like the use of any advanced materials in order to improve the sensor performance. Plasmon excitation in the infrared region of the spectrum involves the use of chalcogenide and silicon as high index coupling prism materials. Modeling and performance investigation of chalcogenide and silicon prism based SPR sensor in infrared light have been reported earlier.[6–9] The admittance loci method has been in use for thin film modeling[10] and has also been employed to design plasmonic structures.[11–14] Gupta *et al.* have reported the resonance tuning and sensitivity enhancement by varying prism materials.[15] Studies on the performance of plasmonic sensor utilizing bimetallic alloy films have also been reported.[16,17] Maharana *et al.*[18] theoretically demonstrated the enhancement of the electric field in surface plasmon resonance bimetallic configuration based on chalcogenide prism. Modeling and performance investigation of a nanobioplasmonic sensor comprising of chalcogenide and silicon prism materials using human skin tissue as a bio-sample have been recently reported.[19]

Most of the literature cited above use the bulk metal film without accounting for the characteristics of its constituent nanoparticles and their respective effects on the overall performance of the sensor. Enhancement of SPR sensing signal using spherical gold nanoparticles of sizes 40–80 nm was achieved and demonstrated in Ref. 20 and this enhancement was due to stronger scattering of gold nanoparticles in comparison to absorption. The investigation of the surface plasmon peak response for gold nanoparticles of different shapes and sizes (nanospheres, nanocubes, nanobranches, nanorods, and nanobipyramids) using water-glycerol mixtures of varying volume ratios have been reported by Chen *et al.*[21] An on-chip spectral SPR optical sensor with improved spectral sensitivity using a self assembled array of silver nanoparticles in the gold film has been proposed by Zhang *et al.*[22] Vivid description of the fabrication procedure of uniformly distributed gold nanoparticle film with controllable size by focused ion beam bombardment on thin gold films was provided in Ref. 23. Gold nanoparticles can be used to improve the performance of many optoelectronic devices. GaN-based metal-semiconductor-metal photodetectors covered with gold nanoparticles were fabricated for achieving improved performance of a plasmonic sensor.[24] A plasmonic device consisting of periodic arrays of ellipsoidal silver nanoparticles embedded in SiO_2 was placed near a silver surface and by tuning the shape of the particles in the array, the nanoparticle surface plasmon resonance is tuned, which in turn excite surface plasmons on the metal film.[25]

[a)]Author to whom correspondence should be addressed. Electronic mail: mraphy@caluniv.ac.in

In the context of the present scenario in this research field, we report a design methodology based on the admittance loci method to design and analyze such nanoparticle based plasmonic sensor. The main emphasis is given to the role played by the different size of spherical shaped gold nanoparticle as well as the use of high index silicon and chalcogenide (commonly known as 2S2G; composition: $Ge_{20}Ga_5Sb_{10}S_{65}$) prism materials with operating wavelength of 1200 nm. Chalcogenide glasses consist of group VI chalcogen elements (sulfur, selenium, and tellurium) generally known for their better thermal stability and chemical reactivity.[26] On the other hand, silicon is a semiconductor material, which is transparent throughout the infrared range. The development of 2S2G and silicon prism material based plasmonic sensors requires the determination of the SPR condition in infrared taking into account the dispersion effects of these materials, which are crucial in the infrared range. The advantage of such a plasmonic sensor is the utilization of high index prism materials like silicon, 2S2G materials along with gold nanoparticle film in one single structure. Moreover, SPR curve width can be controlled in infrared by using high index prism materials and also by changing gold nanoparticle sizes, thus utilizing higher chemical stability of gold (Au) nanoparticles, higher sensitivity offered by 2S2G, and higher detection accuracy (DA) provided by silicon prism materials.

II. MATHEMATICAL BACKGROUND

A. Admittance loci based design method

The admittance loci method is quite well known technique usually employed for designing multilayer thin film structures. We can consider that the multilayer is gradually built up layer by layer, immersed all the time in the ambient medium. As thickness of each layer increases from zero value to its final value, the admittance of the multilayer at that stage of its construction is calculated and locus is plotted. Alternatively, we can assume that the multilayer structure is already constructed and a virtual reference plane is sliding continuously through the layers and the locus of admittance of the structure up to that plane is plotted. This plot is known as the admittance diagram or admittance locus plot.[10]

A plasmonic sensor can be designed using the admittance loci method. According to this method, the admittance of a plasmonic structure is considered, which starts from the sample and ends at the front surface of the structure. Fig. 1 represents a plasmonic structure consisting of prism, gold nanoparticle film, and sample with refractive indices represented by n_{pr}, n_m, and n_{sample}, respectively.

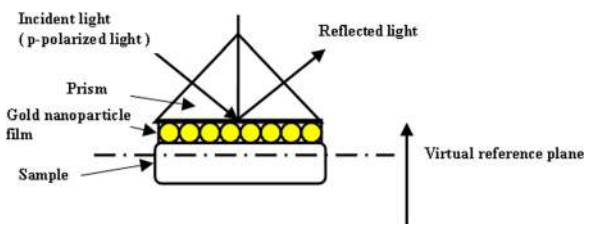

FIG. 1. Schematic diagram of plasmonic structure with gold nanoparticle film (not to scale).

The dielectric constant of gold at different wavelengths has been calculated using the Drude model as

$$\varepsilon_m(\lambda) = 1 - \frac{\lambda^2}{\lambda_p^2\left(1 + i\frac{\lambda}{\lambda_c}\right)}, \tag{1}$$

where λ_p and λ_c is the plasma wavelength and collision wavelength, respectively.

It is to be noted that some metals have contribution from bound electrons, which provide a weak oscillatory behavior due to the frequency dependence of the reflection coefficient,[26] and such metals follows the Lorentz-Drude model.

The inverse of collision wavelength as a function of particle size ($R_{particle}$) is given by

$$\frac{1}{\lambda_c(R_{particle})} = \frac{1}{\lambda_c(bulk)} + \frac{v_f}{2\pi c R_{particle}}, \tag{2}$$

where λ_c ($bulk$) is the bulk collision wavelength, c is the velocity of light in free space, and v_f is the Fermi velocity. The values of plasma wavelength, bulk collision wavelength, and Fermi velocity of gold are taken from literature.[16]

The phase introduced by the gold nanoparticle film of thickness d_m is given by

$$\delta_m = \left(\frac{2\pi}{\lambda}\right) d_m \left(n_m^2 - k_m^2 - n_{pr}^2 \sin^2\theta_i - 2in_m k_m\right)^{1/2}, \tag{3}$$

where n_m and k_m are the real and imaginary part of the complex refractive index of the gold nanoparticle film, n_{pr} is the refractive index of the incident medium (prism material), and λ is the wavelength of incident light.

The characteristic matrix of gold nanoparticle film is given by[10]

$$\begin{bmatrix} B \\ C \end{bmatrix} = \begin{bmatrix} \cos\delta_m & (i\sin\delta_m)/\eta_m^p \\ i\eta_m^p \sin\delta_m & \cos\delta_m \end{bmatrix} \begin{bmatrix} 1 \\ \eta_{sample}^p \end{bmatrix}, \tag{4}$$

where B and C are the normalized electric and magnetic fields at prism-gold nanoparticle film interface.

For gold nanoparticle film, the modified admittances are given by

$$\eta_m^s = \frac{\left(n_m^2 - k_m^2 - n_{pr}^2 \sin^2\theta_i - 2in_m k_m\right)^{1/2}}{\cos\theta_i}, \tag{5}$$

$$\eta_m^p = \frac{(n_m - ik_m)^2}{\eta_m^s}, \tag{6}$$

where the superscripts s and p denote polarization states of the incident light.

For sample, the modified admittance is given by

$$\eta_{sample}^p = \frac{y_{sample}\cos\theta_i}{\cos\theta_{sample}}, \tag{7}$$

where the optical admittance of the sample is $y_{sample} = n_{sample} y_f$, n_{sample} is the refractive index of the sample, y_f is the free space optical admittance, and θ_{sample} is the angle corresponding to the sample.

So, we can write the admittance of a plasmonic sensor as

$$Y = \frac{C}{B} = \frac{\eta^p_{sample} \cos\delta_m + i\eta^p_m \sin\delta_m}{\cos\delta_m + i\left(\frac{\eta^p_{sample}}{\eta^p_m}\right)\sin\delta_m}. \quad (8)$$

The reflectance of a plasmonic sensor is given by

$$R = \left(\frac{\eta_{pr} - Y}{\eta_{pr} + Y}\right)\left(\frac{\eta_{pr} - Y}{\eta_{pr} + Y}\right)^*, \quad (9)$$

where * denotes the complex conjugate.

B. Sensing principle of a plasmonic sensor

Plasmonic devices are mainly based on Kretschmann's Attenuated Total Internal Reflection (ATIR) configuration.[2] In a plasmonic device, a thin plasmon active metal film is deposited on the base of a prism and the p-polarized incident light excites a surface plasmon wave (SPW), which propagates along the metal–dielectric sample interface under the condition that propagation constant of incident light and SPW match. The resonance condition is proposed by Homola *et al.*[4] as given by

$$Kn_{pr}\sin\theta_{SPR} = K\sqrt{\frac{(\varepsilon_{mr} + i\varepsilon_{mi})n^2_{sample}}{(\varepsilon_{mr} + i\varepsilon_{mi}) + n^2_{sample}}}, \quad (10)$$

where ε_m is the complex dielectric constant of the metal, ε_{mr} is the real part, ε_{mi} is the imaginary part of ε_m, and K is the free space wave number.

Here, the right hand term is the real part of the SPW propagation constant, whereas the term on the left hand side is the propagation constant of the p-polarized light incident at an SPR angle through the light coupling prism. The matching of the propagation constants leads to the resonant excitation of SPW, and thereby, a sharp dip in reflectance at the SPR angle is observed. Any change in refractive index of the sample in contact with the metal layer results in the shift of the SPR angle in order to satisfy the SPR condition, under a fixed operating wavelength.

C. Plasmonic sensor performance parameters

The full width at half maximum (FWHM) of an SPR sensing curve is defined as the angular (or spectral) width of the SPR reflectance curve at half the value of maximum reflectance for angular (or spectral) interrogation mode. The performance of a plasmonic sensor is expressed in terms of shift in SPR angle for a small change in sample refractive index values and in terms of the FWHM of the SPR sensing curves, which should be as low as possible in order to accurately determine the SPR dip position. SPR angle is the angle at which reflectance of a plasmonic sensor becomes minimum.

The sensitivity of a plasmonic sensor under consideration is given by[15]

$$S = \frac{d\theta_{SPR}}{dn_{sample}} = \frac{\left(\frac{\varepsilon_{mr}}{\varepsilon_{mr} + n^2_{sample}}\right)^{3/2}}{\sqrt{n^2_{pr} - \frac{\varepsilon_{mr} n^2_{sample}}{\varepsilon_{mr} + n^2_{sample}}}}, \quad (11)$$

where $d\theta_{SPR}$ is the change in SPR angle corresponding to small change in the sample refractive index dn_{Sample}.

SPR angle changes with change in sample refractive index values, so the larger change in SPR angle corresponds to higher sensitivity.

The DA of a plasmonic sensor is defined as the reciprocal of FWHM as given by

$$DA = \frac{1}{FWHM}. \quad (12)$$

Thus, plasmonic sensors, which produce narrower SPR sensing curves (lower value of FWHM), display higher detection accuracy and vice versa. So, the performance criteria of a plasmonic sensor should be based on higher dynamic range and sensitivity or higher detection accuracy as per the sensing requirements.

Accommodating both parameters (sensitivity as well as detection accuracy), the figure of merit (FOM) of a plasmonic sensor can be defined as

$$FOM = \left(\frac{d\theta_{SPR}}{dn_{sample}}\right) \times DA. \quad (13)$$

III. SIMULATION RESULTS AND DISCUSSION

A. Admittance loci design plots based on gold nanoparticle sizes

The admittance loci plots for structures using spherical shaped gold nanoparticle film having the particle size of 6 nm with silicon and 2S2G as prism materials, and dielectric sample having a refractive index (RI) of 1.33 at 1200 nm wavelength of light are shown in Fig. 2(a). From this admittance loci plots, it can be interpreted for silicon prism that initially starting admittance of the gold nanoparticle film stays on the imaginary axis, with the locus point moving from the coordinate (0, 5.278i) on the imaginary axis (which corresponds gold nanoparticle film thickness of 0 nm) and intercepts the real admittance axis at 3.529 (which is close to refractive index of silicon prism, 3.525 at 1200 nm) for gold nanoparticle film thickness of 32 nm. For an angle of incidence of 22.79°, it also yields near-zero reflectance with this specific gold nanoparticle film thickness. If this locus could have been made to intercept the real axis of the admittance diagram exactly at the refractive index of the incident medium (prism material), the surface plasmon excitation would have been achieved with much better efficiency. In a similar

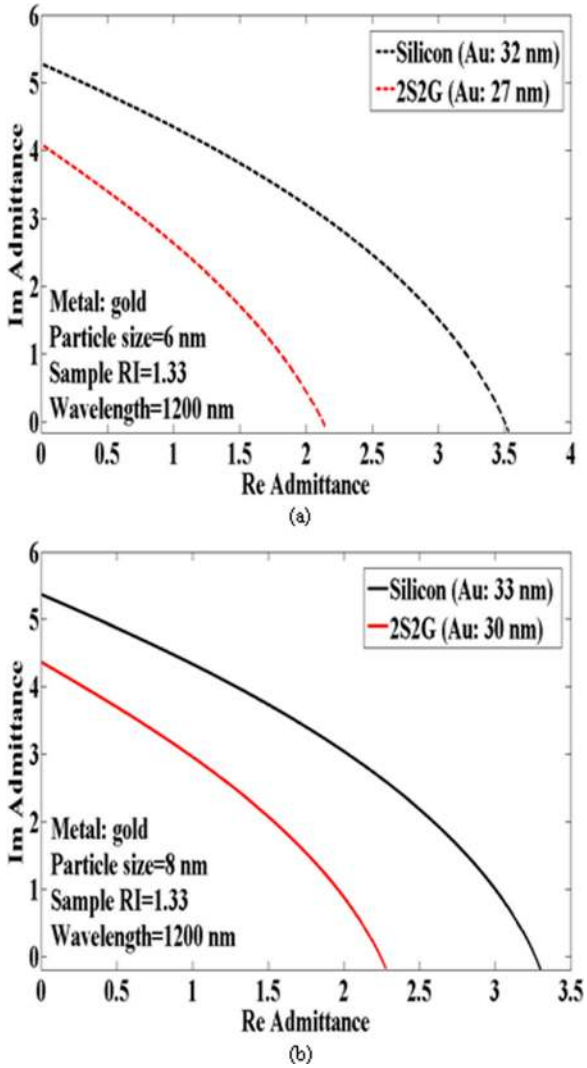

FIG. 2. Admittance loci plots of a 2S2G and silicon prism based plasmonic sensor for gold nanoparticle sizes of (a) 6 nm and (b) 8 nm.

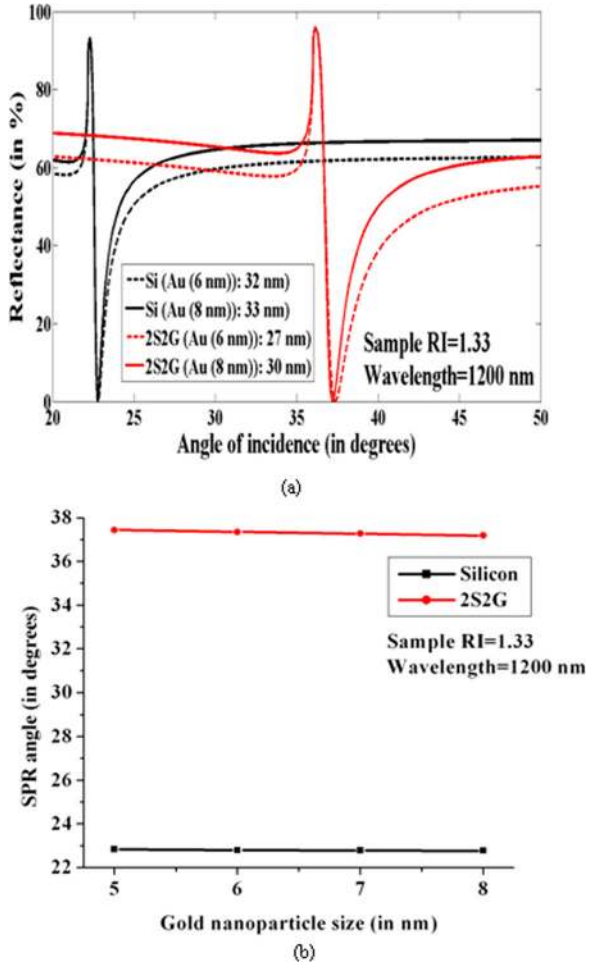

FIG. 3. (a) SPR curves of a plasmonic sensor using silicon and 2S2G as prism materials for gold nanoparticle sizes of 6 nm and 8 nm, respectively, and (b) SPR angle plot with variation of gold nanoparticle sizes using silicon and 2S2G prism materials.

manner, Fig. 2(b) depicts the admittance loci plots for silicon and 2S2G prism with the gold nanoparticle size of 8 nm.

The refractive indices of silicon and 2S2G prism materials are taken as 3.525 and 2.2631 at 1200 nm wavelength in infrared in accordance with our previous article.[9] The calculated values of starting imaginary admittance, end admittance, and incident angle for each prism material are tabulated in Table I. In all these cases, we have optimized gold nanoparticle film thickness of each prism material so as to ensure that the respective loci end with a real admittance value close to the refractive index of the prism for an efficient excitation of surface plasmons.

B. Surface plasmon sensing curves

Fig. 3(a) shows the SPR curves for silicon and 2S2G prism materials with gold nanoparticle sizes of 6 nm and 8 nm, respectively. Here, the sample refractive index (RI) value is kept at 1.33. Gold metal film thicknesses have already been optimized for silicon and 2S2G prism materials in order to obtain minimum reflectance. Minimum reflectance actually implies the coupling of maximum energy from incident light to surface plasmons according to the principle of conservation of energy. From our simulated curves, it is seen that silicon material produces a narrower SPR curve than 2S2G material in infrared and also silicon prism based sensor operates at low incident angle region than 2S2G prism

TABLE I. Admittance related parameters for Silicon and 2S2G prism based sensor.

Prism material	Gold nanoparticle size (nm)	Thickness of gold metal film (nm)	Starting imaginary admittance	End admittance	Angle of incidence (degrees)
Silicon	6	32	5.278i	3.529, −0.1454i	22.79
	8	33	5.366i	3.298, −0.1917i	22.77
2S2G	6	27	4.094i	2.141, −0.06071i	37.37
	8	30	4.366i	2.275, −0.1767i	37.21

based sensor. It can also be observed that the shift in SPR dip position with a change in nanoparticle sizes is less prominent for silicon as compared to 2S2G.

Fig. 3(b) shows the plot of SPR angle with variation in gold nanoparticle sizes for silicon and 2S2G prism materials. It is seen that SPR angle is higher for 2S2G material and lower for silicon material. Moreover, the SPR angle remains almost constant with gold nanoparticle size variation.

Fig. 4 shows simulated plots of SPR sensing curves for silicon prism and gold nanoparticle film (nanoparticle size: 8 nm and optimized film thickness: 33 nm) with different weights (in %) of glycerol in water solution as the sample. For simulation, different weights of glycerol in glycerol-water solution and their corresponding refractive index values at 20 °C were taken from data presented in Ref. 27. From these curves, one can observe that change in weight (in %) of glycerol in glycerol-water solution provides a change in refractive index of the sample, which actually tunes the SPR dip position.

C. Performance parameter issues based on gold nanoparticle sizes

The sensitivity can be theoretically evaluated using Eq. (11). The FWHM is an important factor to be considered for the actual design of a plasmonic sensor. Another important parameter is the dynamic range, which is defined as the range of dielectric samples which can be sensed as governed by surface plasmon resonance condition. The maximum value of the refractive index of the sample that can be sensed by a particular plasmonic sensor can be obtained using Eq. (10) when $\sin(\theta_{SPR})$ is just less than unity.[15] With silicon prism and Au metal (Au nanoparticle size = 6 nm), at 1200 nm wavelength, the sample refractive index for which $\theta_{SPR} = 90^{o}$ was calculated to be $(n_{sample})_{\max} = 3.1284$. So, with Au metal having nanoparticle size of 6 nm and silicon prism at 1200 nm wavelength, all the dielectric samples having refractive indices less than 3.1284 are detectable. Similarly, for 2S2G prism material, this limit is 2.1470 for gold nanoparticle size of 6 nm. Figs. 5(a) and 5(b) show the plots of dynamic range and sensitivity with variation in gold nanoparticle sizes for silicon and 2S2G prism materials. It is seen that the dynamic range is higher for silicon material and lower for 2S2G material. But on the other hand, sensitivity is higher for 2S2G material and lower for silicon material. Moreover, the dynamic range and sensitivity remain almost constant with gold nanoparticle size variation, because of the fact that real part of gold metal dielectric constant does not vary much with gold nanoparticle size. So, one should choose the correct value of gold nanoparticle size and proper prism material depending on the application concerned with a compromise between the sensitivity and the dynamic range requirements.

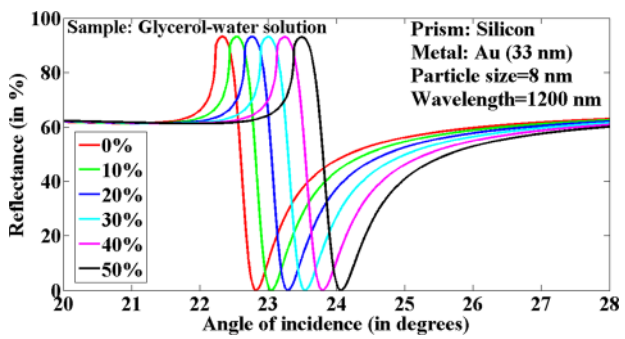

FIG. 4. SPR curves of a plasmonic sensor using silicon prism material, gold nanoparticle size of 8 nm, and different weights (in %) of glycerol (as shown in the legend) in water solution as the sample.

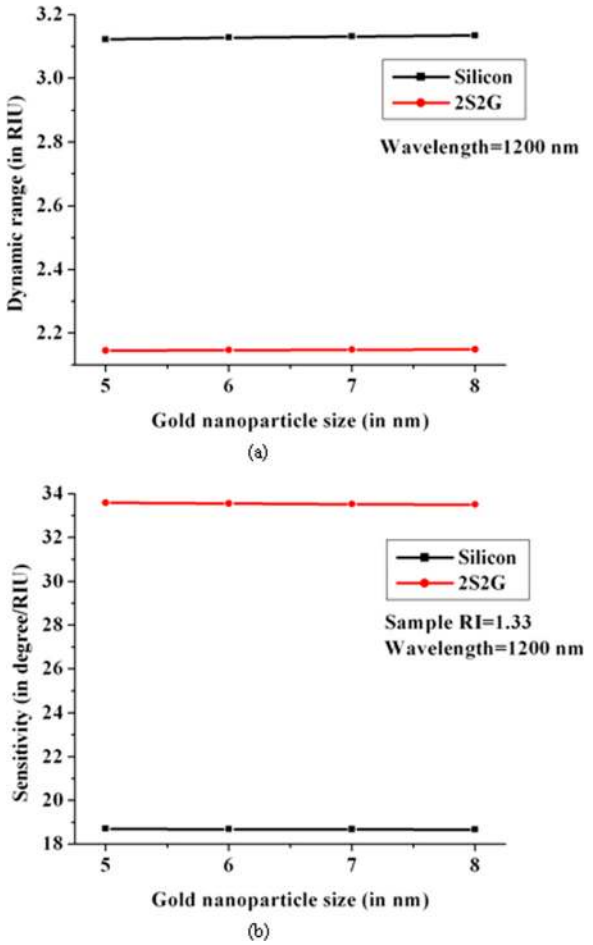

FIG. 5. Plots of (a) dynamic range and (b) sensitivity vs. gold nanoparticle sizes for silicon and 2S2G prism materials with sample RI = 1.33.

Moreover, we can compare this gold nanoparticle based plasmonic structure to plasmonic structure reported earlier in literature[9] in terms of sensitivity. While evaluating sensitivity, complex refractive index of gold nanoparticle film was calculated in terms of nanoparticle size using Eqs. (1) and (2), and the complex refractive index of the normal gold film was obtained from the literature.[9] Fig. 6(a) shows sensitivity plots for silicon and 2S2G prism materials using gold nanoparticle film (gold nanoparticle size = 8 nm) and normal gold film coating using the analytical expression of Eq. (11). The simulated sensitivity plots suggest that the gold nanoparticle film based plasmonic sensor shows higher sensitivity than the conventional gold film based plasmonic sensor for both prism materials used. Fig. 6(b) shows the variation of sensitivity expressed as degree per glycerol weight (in %) with change in glycerol weight (in %) in glycerol-water solution

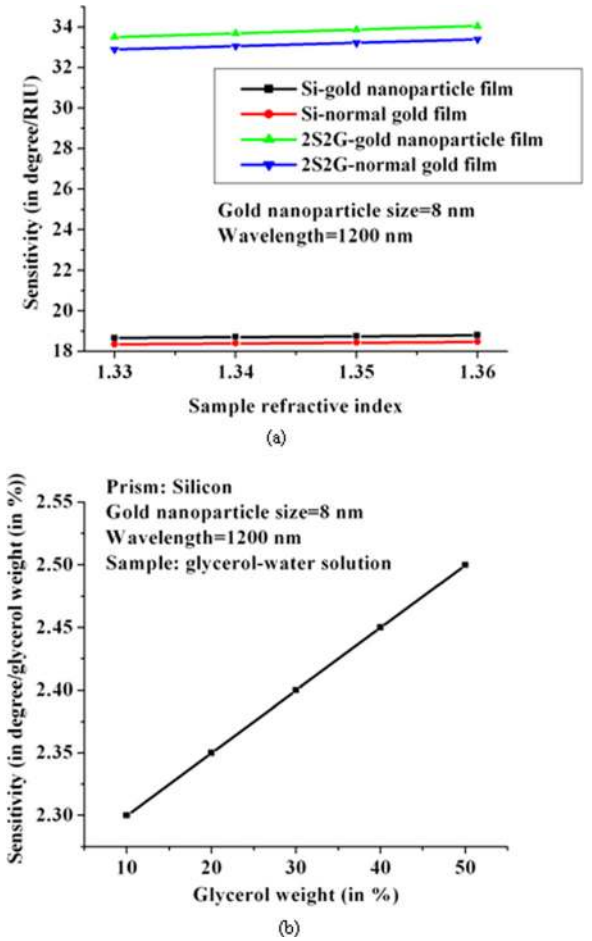

FIG. 6. (a) Sensitivity vs. sample refractive index plot for silicon and 2S2G prism materials with normal gold film and gold nanoparticle film with nanoparticle size of 8 nm and (b) plot of sensitivity vs. glycerol weight (in %) for silicon prism material and gold nanoparticle film with nanoparticle size of 8 nm.

at 20 °C for silicon prism material using gold nanoparticle film (gold nanoparticle size: 8 nm). It is seen that as weight (in %) of glycerol in glycerol-water solution increases, sensitivity also increases. It is to be noted that the calculation of the sensitivity in this case is carried out numerically considering the water (i.e., 0% glycerol weight) as a reference sample.

The real part of end admittance value can be obtained from simulated admittance loci plot and according to the principle of efficient plasmonic excitation, the real part of end admittance value should be close to the refractive index of the prism material used as mentioned before, and it was found that our calculated real part of end admittance value for silicon prism with 6 nm gold nanoparticle size was in close agreement with the refractive index of silicon prism material at 1200 nm wavelength. So, for efficient plasmonic excitation point of view, in place of actual prism material refractive index, real part of end admittance value can be used, and using this calculated end admittance value, dynamic range has been calculated for silicon prism material with 6 nm gold nanoparticle size as shown in Table II. For comparison, the dynamic range has also been calculated using the actual refractive index of silicon prism material. It is

TABLE II. Dynamic range and sensitivity data at 1200 nm wavelength with 6 nm gold nanoparticle size.

Prism material	$DR^{a}_{RPEA}{}^{b}$ (RIU)	$DR_{PMRI}{}^{c}$ (RIU)	S_{RPEA} (degree/RIU)	S_{PMRI} (degree/RIU)
Silicon	3.1312	3.1284	18.6591	18.6839

[a]DR: dynamic range
[b]RPEA: real part of end admittance
[c]PMRI: prism material refractive index

seen that the dynamic range value, based on the real part of end admittance value, was in close agreement with that obtained using actual value of the prism material refractive index at 1200 nm wavelength. Table II also shows the calculated values of sensitivity at 1200 nm wavelength for silicon as the coupling prism material with 6 nm gold nanoparticle size and sample of refractive index 1.33. Sensitivity (as shown in Eq. (11)) was calculated using real part of end admittance value (using the admittance approach) and side by side using an actual refractive index of prism material. It is seen that both approaches provide the sensitivity values, which are in close agreement.

Figs. 7(a) and 7(b) show the plots of FWHM and detection accuracy with variation of gold metal nanoparticle sizes. It can be observed that FWHM decreases as nanoparticle size increases, whereas detection accuracy increases with increase in gold nanoparticle size. FWHM was also calculated using actual values of prism material refractive indices and real part of end admittance values. It was found that with silicon prism and gold nanoparticle size of 6 nm, the FWHM value based on the real part of end admittance value was 2.35°, whereas that based on the actual value of the prism material refractive index was 2.38°. So, it can be seen that calculated FWHM values are also in close agreement. From Eq. (2), it can be concluded that the increase in gold nanoparticle size leads to increase in the collision wavelength followed by a decrease in the imaginary (absorption) part of the surface plasmon propagation constant (R.H.S. expression of Eq. (10)). As the imaginary part of the surface plasmon propagation constant corresponds to the absorption of light power by the surface plasmon sensing region, it implies that the fraction of light power absorbed is inversely proportional to the size of gold metal nanoparticles. As a result, reflectance increases, causing SPR curve to broaden (larger FWHM) with a decrease in gold nanoparticle size. It is also clear that FWHM is higher for 2S2G prism material and lower for silicon prism material. So, larger nanoparticle size along with silicon prism ensures precise determination of SPR dip position resulting in more accurate infrared SPR sensing.

The dip depth of a surface plasmon sensing curve is defined as the difference between the maximum and minimum value of the reflectance of SPR curve. The dip depth, FOM, plots as a function of variation of gold nanoparticle sizes have been shown in Figs. 8(a) and 8(b). It is seen that dip depth and FOM both increase with increase in gold nanoparticle size, though dip depth is higher for silicon material and lower for 2S2G material. On the other hand, FOM is higher for silicon material and lower for 2S2G material due

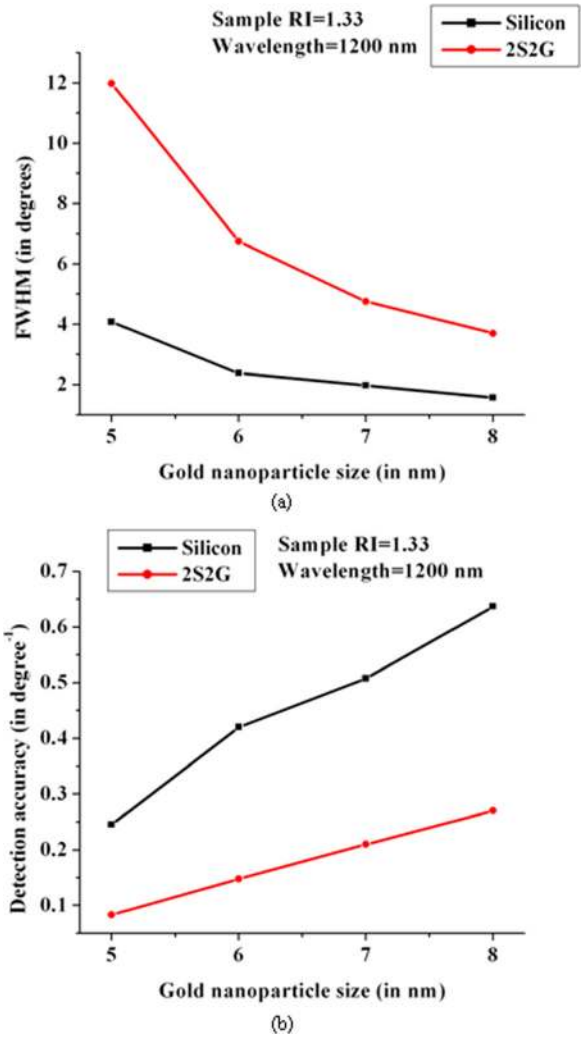

FIG. 7. Plot of (a) FWHM and (b) detection accuracy vs. gold nanoparticle sizes with sample RI = 1.33 for silicon and 2S2G prism materials.

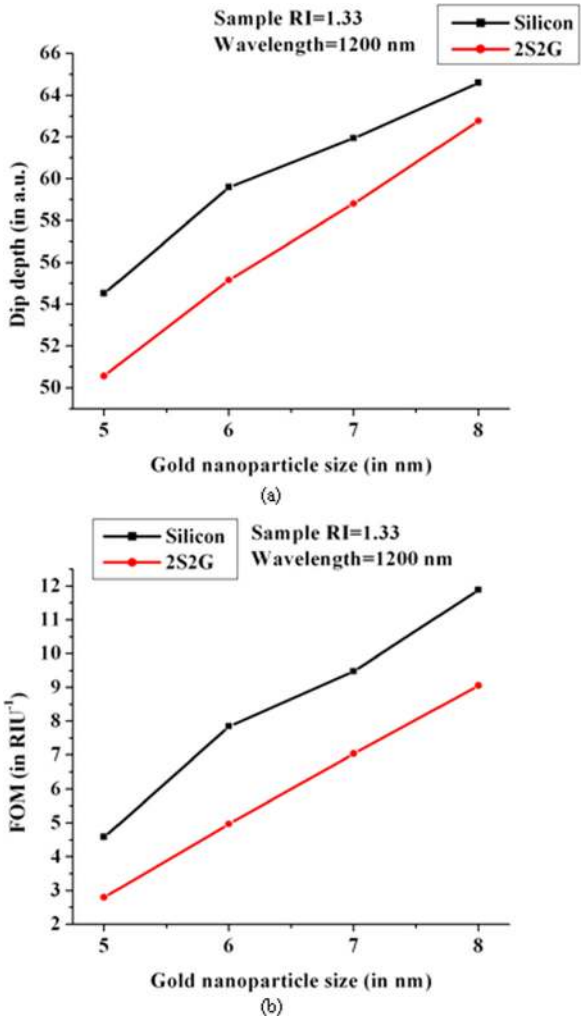

FIG. 8. Plot of (a) Dip depth and (b) FOM vs. gold nanoparticle sizes with sample RI = 1.33 for silicon and 2S2G prism materials.

to narrower SPR curves of silicon compared to 2S2G prism based structures.

The proposed gold nanoparticle based configuration is advantageous, as it has an additional degree of freedom, namely, gold nanoparticle size. Apart from changing refractive indices of prism materials and thickness of gold nanoparticle coating, one can also change gold nanoparticle size. By changing nanoparticle sizes, thicknesses, and refractive indices of prism materials, the SPR dip position and SPR curve width can be tuned and controlled, which can significantly affect the performance of the sensor. Whereas conventional prism based plasmonic configuration using a normal gold coating has only two degrees of freedom, namely, the metal film thickness and refractive index of prism material.

IV. CONCLUSION

We theoretically investigate the effect of gold nanoparticle size and high index prism material on the performance of a plasmonic sensor using the admittance loci method in infrared light. In this work, we have considered two different high index prism materials and different nanoparticle sizes of gold nanoparticle film in order to see the effect of these parameters on admittance loci plots of the plasmonic sensor as well as on SPR sensing curves. We have also studied various parameters related to SPR sensing, namely, SPR angle, sensitivity, figure of merit, dynamic range, dip depth, FWHM, and detection accuracy. These parameters are found to be greatly influenced by the refractive index of high index prism material and gold nanoparticle size. The choice of prism materials and nanoparticle size of gold must be in accordance with the application concerned, keeping in mind the optimized trade-off among the sensitivity, FWHM, and dynamic range requirements. The use of silicon in the design of plasmonic sensors provides the advantage of microfabrication in order to aid in miniaturization and integration of a plasmonic sensor. 2S2G prism material sensors, on the other hand, could provide better performance due to its wide transparency range starting from visible to infrared region of the spectrum. These sensors have applications in field of sensing, environmental analysis, and many more. Our work could provide a platform for further research in infrared plasmonic sensor design, and our method of approach could be advantageous as a pre-fabrication design requirement of an efficient plasmonic sensor.

ACKNOWLEDGMENTS

The authors wish to acknowledge the Centre for Research in Nanoscience and Nanotechnology (CRNN), University of Calcutta, Kolkata, India. Kaushik Brahmachari is grateful to Technical Education Quality Improvement Programme (TEQIP PHASE II), University College of Technology, University of Calcutta, for awarding Senior Research Assistantship to carry out this work.

[1]A. Otto, Z. Phys. **216**, 398 (1968).
[2]E. Kretschmann and H. Raether, Z. Naturforsch., A: Phys. Sci. **23A**, 2135 (1968).
[3]B. Liedberg, C. Nylander, and I. Lunström, Sens. Actuators **4**, 299 (1983).
[4]J. Homola, I. Koudela, and S. S. Yee, Sens. Actuators, B: Chemical **54**, 16 (1999).
[5]M. A. Ordal, L. L. Long, R. J. Bell, S. E. Bell, R. R. Bell, R. W. Alexander, Jr., and C. A. Ward, Appl. Opt. **22**, 1099 (1983).
[6]J. Le Person, F. Colas, C. Compère, M. Lehaitre, M.-L. Anne, C. Boussard-Plèdel, B. Bureau, J.-L. Adam, S. Deputier, and M. Guilloux-Viry, Sens. Actuators, B: Chemical **130**, 771 (2008).
[7]S. Patskovsky, A. V. Kabashin, M. Meunier, and J. H. T. Luong, Sens. Actuators, B: Chemical **97**, 409 (2004).
[8]S. Patskovsky, A. V. Kabashin, M. Meunier, and J. H. T. Luong, J. Opt. Soc. Am. A **20**(8), 1644 (2003).
[9]K. Brahmachari and M. Ray, Opt. Eng. **52**(8), 087112-1 (2013).
[10]H. A. Macleod, *Thin-Film Optical Filters*, 4th ed. (Taylor & Francis Group, New York, 2010).
[11]C. W. Lin, K. P. Chen, M. C. Su, C. K. Lee, and C. C. Yang, Opt. Quantum Electron. **37**, 1423 (2005).
[12]C. W. Lin, K. P. Chen, M. C. Su, T. C. Hsiao, S. S. Lee, S. Lin, X. J. Shi, and C. K. Lee, Sens. Actuators, B: Chemical **117**, 219 (2006).
[13]Y. J. Jen, A. Lakhtakia, C. W. Yu, and T. Y. Chan, J. Opt. Soc. Am. A **26**(12), 2600 (2009).
[14]K. Brahmachari and M. Ray, Sens. Actuators, A: Phys. **212**, 102 (2014).
[15]G. Gupta and J. Kondoh, Sens. Actuators, B: Chemical **122**, 381 (2007).
[16]A. K. Sharma and G. J. Mohr, J. Phys. D: Appl. Phys. **41**, 055106 (2008).
[17]A. K. Sharma and R. Jha, J. Appl. Phys. **106**, 103101 (2009).
[18]P. K. Maharana, S. Bharadwaj, and R. Jha, J. Appl. Phys. **114**, 014304-1 (2013).
[19]K. Brahmachari and M. Ray, Sens. Actuators, B: Chemical **208**, 283 (2015).
[20]S. Zeng, X. Yu, W. C. Law, Y. Zhang, R. Hu, X.-Q. Dinh, H.-P. Ho, and K.-T. Yong, Sens. Actuators, B: Chemical **176**, 1128 (2013).
[21]H. Chen, X. Kou, Z. Yang, W. Ni, and J. Wang, Langmuir **24**, 5233 (2008).
[22]W. Zhang, W. Ye, C. Wang, W. Li, Z. Yue, and G. Liu, Micro Nano Lett. **9**, 585 (2014).
[23]X. Zhou, Q. Wei, K. Sun, and L. Wang, Appl. Phys. Lett. **94**, 133107 (2009).
[24]Z. D. Huang, W. Y. Weng, S.-J. Chang, Y.-F. Hua, C.-J. Chiu, and T.-Y. Tsai, IEEE Photonics Technol. Lett. **25**, 1809 (2013).
[25]A. Ghoshal and P. G. Kik, J. Appl. Phys. **103**, 113111 (2008).
[26]J. H. Simmons and K. S. Potter, *Optical Materials* (Academic Press, CA, 2000).
[27]E. Jungermann and N. O. V. Sonntag, *Glycerine: A Key Cosmetic Ingredient* (Marcel Dekker, New York, 1991).